

## HEAT TRANSFER AND PRESSURE DROP DURING CONDENSATION OF R134a INSIDE TWO MICRO-FIN TUBES OF NEW DESIGN

Luigi Colombo, Adriano Muzzio, Alfonso Niro

Dipartimento di Energetica, Politecnico di Milano, I-20133 Milano, Italy

### ABSTRACT

This paper presents experimental data on heat transfer coefficients and pressure drops during convective condensation of oil-free R134a inside two 9.52-mm micro-fin tubes of new design and in a smooth tube with the same outside diameter. All the tubes are horizontally operated. The two micro-fin tubes are characterized by 54 and 82 sharp fins alternating with two different heights, that is the distinguishing feature from other new micro-fin tubes. The effects of mass flux, average quality and overall quality change on heat transfer characteristics have been separately investigated. The data here reported are for a nominal temperature of 35 °C, with mass flux ranging from 90 to 400 kg/s m<sup>2</sup>, inlet quality from 0.8 to 0.4 and quality change between 0.6 and 0.2. Finally, experimental data on heat transfer and pressure drop for one of the micro-fin tubes are compared to predictions of some recent correlations specifically proposed for condensation of conventional and alternative refrigerants inside micro-fin tubes.

### INTRODUCTION

The design of high performance compact heat exchanger led to develop many types of extended surfaces. In refrigeration and air-conditioning applications, reduction of the air-side thermal resistance to the refrigerant-side values urged industry to focus on enhancing heat transfer during in-tube evaporation and condensation. Among enhancement techniques, micro-fin tubes are widely used because of their high heat transfer performance with moderate pressure drop increase. Micro-fin tubes are characterized by numerous small fins that spiral down the inside surface, and they were first reported in the open literature in the mid 1970's. In the subsequent years, an increasing number of additional papers on boiling and condensation of refrigerants inside these tubes have been published. Comprehensive reviews of the previous works are reported by Schlager et al. [1,2] and Webb [3]. Among these are Schlager et al. [4] who reported R22 evaporation and condensation coefficients and pressure drop for three 12.7 mm outside diameter micro-fin tubes having different helix angles. However, their tubes also had different fin heights (ranging from 0.15 to 0.3mm) and pitches, and they did not define the effect of specific geometry factors on the performance differences. The effect of geometry factors was considered by Yasuda et al. [5] who investigated the condensation coefficients and pressure drop for 9.52 mm outside diameter micro-fins tubes with different fin height, number of fins and helix angles. They reported that the condensation heat transfer coefficient increases with groove depth and helix angle. They also reported an optimum number of grooves between 55 and 60 for the 9.52 mm diameter tube. Chiang [6] tested four micro-fin tubes having different axial and helical grooves using R22 as the working fluid. He reported that the condensation heat transfer coefficient for an axial grooved tube is higher than for 18° helical

grooves for equal tubes diameters. However, the tested tubes had different fin height and apex angle, which both have significant effect on the condensation heat transfer coefficient.

Although considerable evaporation and condensation data have been published, very little work has been done to explain the enhancement mechanism for condensation or evaporation in the micro-fin tube. While vapour shear force should be a dominant factor in establishing the performance, Webb [3] proposes that surface tension force should also be important for condensation on the fins. However, no data have yet been published that verifies this possibility.

More recently, international regulations banned the use of CFCs like R12 and imposed phase-out schedules on the production of HCFCs like R22. Consequently, an extensive search for potential replacements has been made during the past decade. R134a was the first alternative refrigerant and may be designated today as state-of-art; in its physical and refrigeration properties, it compares very well to R12.

The appearance of refrigerant substitutes redirected research on micro-fin tubes towards testing their heat transfer characteristics with these new fluids. References [7,14] are a sample of the many papers recently published on these investigations. However, evaporation and condensation of alternative refrigerants inside micro-fin tubes have not been thoroughly surveyed yet and there is a large demand for further experimental research.

This paper presents experimental data on convective condensation of R134a in two micro-fin tubes of new design developed by Trefimetaux, as well in a smooth tube for comparison. Pressure drop data are also reported. The data show the effects of mass velocity, vapor quality and heat flux on thermal performances of R134a inside these micro-fin tubes. Finally, experimental data on heat transfer and pressure drop for one of the micro-fin tubes are compared to predictions of some

recent correlations specifically proposed for condensation of conventional and alternative refrigerants inside micro-fin tubes.

## EXPERIMENTAL APPARATUS

A schematic diagram of the experimental facility is shown in Figure 1. The apparatus is composed of three independent circuits, namely, a refrigerant circuit, a heating/cooling water circuit and a chilled coolant (water-glycol solution) circuit.

The refrigerant circuit mainly consists of a boiler, the test section, a condenser, a gear pump and a filter dryer. Liquid and vapor are drawn from the boiler through two distinct lines. A subcooler and a mass flow-meter are mounted on the liquid

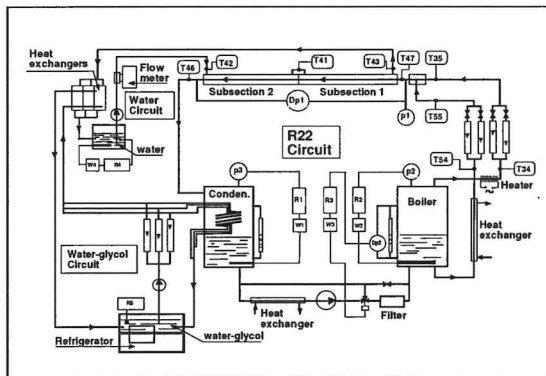


Figure 1. Schematic diagram of the experimental facility.

line whereas a superheater and two float-type flow-meters are installed on the other line. Subcooler and superheater ensure a single-phase flow through the flow-meters for any operating conditions. The liquid and vapor flow rates are controlled by precision metering valves. Downstream of the valves, vapor and liquid streams are mixed; the resulting two-phase mixture flows through a 1.5 m long calming section and then it enters the test tube, that is the inner tube of a double-pipe heat exchanger. At the exit, the refrigerant is discharged into a shell-and-coil condenser; a gear pump conveys the refrigerant from the condenser to the boiler. The heating/cooling circuit supplies the water flowing in the annulus outside the test tube. This circuit is composed by a centrifugal pump, a plate heat exchanger and a bath vessel equipped with a 5-kW heater controlling the water temperature. A magnetic flow-meter is used to measure the water flow rate through the test section annulus. Finally, the chilled coolant circuit is filled with a water-glycol solution and it supplies the cold medium circulating into heat exchangers mounted on the refrigerant and water circuits. A commercial refrigeration unit is used as chiller.

The test section is divided into two identical subsections mounted in series; each subsection is 1.3-m long with an effective heat transfer length of 1.12 m, that is the distance between the inlet and outlet ducts of the outside tube. At the inlet of test section, a temperature probe is mounted inside the tube countercurrently to the refrigerant flow. Such a probe consists of a 0.25-mm, K-type thermocouple plugged into a L-shaped, 8-cm long, 2-mm o.d. tube that is located at the centerline of the duct. In addition, at the entrance and exit of the first subsection and at the outlet of the second one, there are two pressure-taps. Downstream the exit pressure taps of each

subsection there is a sight glass made of 85-mm long, 8.5-mm i.d., pyrex smooth tube; sight glasses are neither heated or cooled. Finally, each subsection is equipped with four T-type thermocouples to measure wall temperatures; the thermocouples are placed in pairs on the top and the bottom of the test tube. Each thermocouple is cemented in a longitudinal groove cut in the outside wall of the test tube, with the tip at 140 mm from the tube end and at 50 mm from the inlet/outlet duct of the outside annulus. Calming and test sections are thermally insulated by a 10-cm thick, glass-wool covering that ensures a measured thermal resistance of 4 K/W.

## DATA REDUCTION

Signals from thermocouples and transducers are cyclically read by a data acquisition unit and sent to an on-line PC. In order for all variables to be affected by similar RMS relative errors, the measurements of refrigerant temperature, pressure drop and water flow rate are based on 30, 50 and 100 readings for cycle, respectively. Every experimental value, instead, is obtained by averaging the measurements of ten cycles in order to reduce the influence of random errors and fluctuations. Finally, for every operative condition, more than ten experimental data are collected.

The heat transfer coefficient is computed as follows. We assume the refrigerant temperature varies linearly between the value  $T_{in}$ , measured at the entrance of the test section, and the value  $T_{out}$  computed at the exit as  $T_S(p_S(T_{in}) - \Delta p)$ , where  $T_S$  is the function correlating the saturation temperature to the pressure,  $p_S$  the inverse function of  $T_S$ , and  $\Delta p$  the pressure drop measured along the test section. Then, for each subsection we calculate the mean refrigerant temperature  $T_{r,m,i}$ , the mean wall temperature  $T_{w,m,i}$ , the refrigerant to wall temperature mean difference  $\Delta T_{m,i} = (T_{w,m,i} - T_{r,m,i})$ , and the heat transfer coefficient  $h_i = q_i / \Delta T_{m,i}$  where  $q_i$  is the mean heat flux based on a nominal inside area corresponding to the maximum internal diameter, i.e., the diameter at the root of micro-fins. Eventually, we compute the average heat transfer coefficient for the test section as the arithmetic mean of the subsection coefficients  $h_i$ . Relevant variables for the present investigation are affected by the following representative experimental uncertainties measured or estimated by an error propagation analysis:  $\pm 2.8\%$  for the refrigerant mass flow rate,  $\pm 1.3\%$  for the inlet quality,  $\pm 0.2$  K between the refrigerant temperature and the saturation one,  $\pm 1.0\%$  for the refrigerant pressure drop,  $\pm 1.0\%$  for the water volume flow rate,  $\pm 0.02$  K for the water temperature difference between the subsection inlet and outlet,  $\pm 1.4\%$  for the heat rate, and  $\pm 7\%$  for the average heat transfer coefficient.

## RESULTS AND DISCUSSION

In saturated flow boiling, for a fixed section configuration (shape, dimensions and orientation with respect to gravity), average heat transfer coefficient and pressure drop depend on four independent variables, namely, total mass flow rate, temperature (or pressure), inlet thermodynamic quality and heat rate or quality change over the section, being the fluid everywhere saturated.

The experimental data here reported were obtained with oil-free refrigerant R134a inside two 9.52-mm micro-fin tubes of new design and in a smooth tube with the same outside diameter. The micro-fin tubes were developed and manufactured by Trefimetaux, namely, Metofin 952-30VA40/54 and Metofin

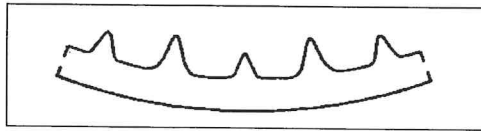


Figure 2. Drawing of the micro-fin cross-section profile.

952-45HVA40/82 which in the following will be indicated by VA and by HVA for the sake of brevity. They are characterized respectively by 54 and 82 sharp fins with an apex angle of 40 degrees, alternating with two different heights as shown in Figure 2. The latter is the distinguishing feature from other new micro-fin tubes. Table 1 lists geometrical parameters of the micro-fin tubes as well as of the smooth tube; the last two parameters give the heat transfer area increase and the cross-section area reduction, respectively, of the microfin-tube with respect to a smooth tube with an internal diameter equal to the maximum inside diameter. Tests were carried out at a nominal temperature of  $308 \pm 0.2$  K, corresponding to a pressure of 0.89 MPa. Total mass flow rate, inlet thermodynamic quality and quality change were varied in turn while keeping the others constant in order to show clearly the effect of each variable against the others. The total mass flow rate ranged from 5.56 to 25 g/s corresponding to a mass flux  $G$ , with respect to a nominal cross-section area based on the maximum internal diameter, that varies between about 90 and 400  $\text{kg/s m}^2$ . The inlet quality  $x_{in}$  was varied from 0.8 to 0.4 whereas the quality change  $\Delta x$  ranges from 0.2 to 0.6.

Figure 3 displays the average heat transfer coefficient  $h_c$  plotted versus the mass flux  $G$  for the micro-fin and smooth tubes; data are for inlet quality  $x_{in}=0.8$  and quality change  $\Delta x=0.6$ . In considering this figure, it is worth noting that mass flux variations at constant  $\Delta x$  imply proportional variations in heat flux due to their linear dependence; for the data reported in figure, the average heat flux ranges from 7.8 to 36  $\text{kW/m}^2$ . As expected, the heat transfer coefficient is an increasing function of  $G$ , but trend for the micro-fin tubes differs from that of the smooth tube. For the latter, data exhibit a linear-at-interval dependence on  $G$  with a change of slope approximately at  $G=250$   $\text{kg/s m}^2$ . Supported by visual observations, we infer that in the first region, where heat transfer is weakly dependent on the mass flux, the flow is stratified whereas it is annular

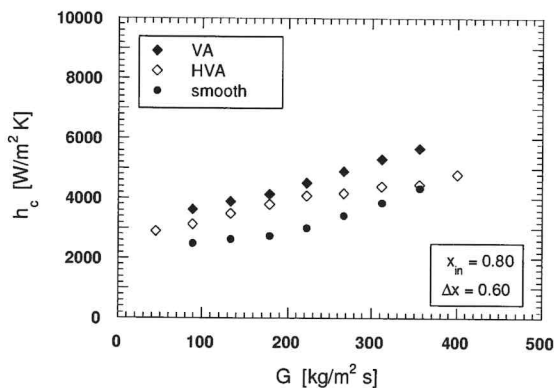


Figure 3. Heat transfer coefficient  $h_c$  versus mass flux  $G$  for fixed inlet quality  $x_{in}$  and quality change  $\Delta x$ .

Parameter	Tube	VA	HVA	smooth
Outside diameter	[mm]	9.52	9.52	9.52
Maximum inside diameter	[mm]	8.92	8.62	8.92
Bottom wall thickness	[mm]	0.30	0.45	0.30
Higher fin height	[mm]	0.23	0.20	-
Lower fin height	[mm]	0.16	0.17	-
Apex angle		40°	40°	-
Number of grooves		54	82	-
Helix angle		18°	18°	-
Inside-surface area ratio		1.58	1.84	1
Actual cross-section area ratio		0.96	0.95	1

Table 1. Geometrical parameters of the tested tubes.

when  $h_c$  starts to increase more steeply with  $G$ . Both the micro-fin tubes exhibit higher values of heat transfer coefficient and data do not display any change of slope marking the transition from stratified to annular flow. Results qualitatively similar to those reported in Figure 3 have been obtained for quality changes of 0.2 and 0.4 while keeping fixed the average quality. We conjecture that in stratified flow microgrooves hold up the condensate at the top of the tube and they promote the formation of a thicker liquid film which in turn lowers the liquid pool. As well known, a redistribution of condensate from the pool to the film yields a higher heat transfer coefficient. On the other hand, in the annular flow microgrooves spread condensate over all the inside surface of the tube thinning the liquid film and increasing heat transfer; however the ratio of the heat transfer coefficient to that of a smooth tube, i.e., the enhancement factor, decreases as mass flux increases. Regarding the comparison between the micro-fin tubes, it is evident that the highest heat transfer coefficients are provided by the VA geometry.

Differences in thermal performances are well accounted by the enhancement factor. A plot of this factor versus  $G$  is shown in Figure 4. As seen, for the VA-tube the enhancement factor is a weakly variable function of the mass flux, with a not very marked maximum of 1.5 at  $G=266$   $\text{kg/s m}^2$  followed by a slight slope down to 1.25; hence, the enhancement factor remains lower than the inside-surface area ratio of this tube

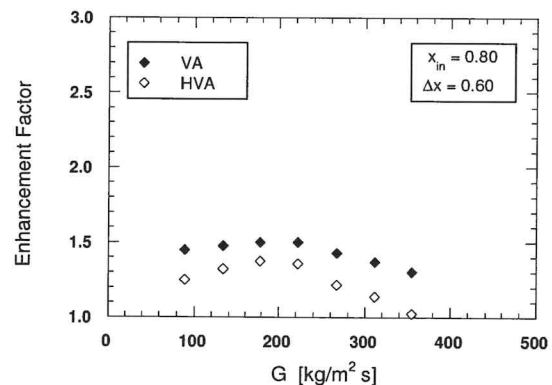


Figure 4. Enhancement Factor versus mass flux  $G$  for fixed inlet quality  $x_{in}$  and quality change  $\Delta x$ .

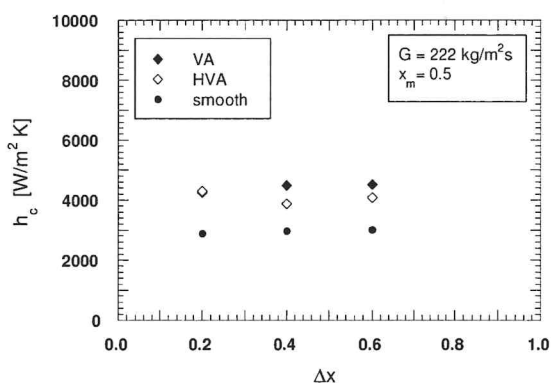


Figure 5. Heat transfer coefficient  $h_c$  versus quality change  $\Delta x$  for fixed mass flux  $G$  and inlet quality  $x_{in}$ .

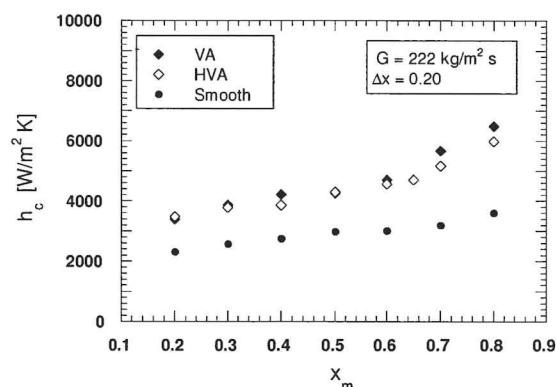


Figure 6. Heat transfer coefficient  $h_c$  versus average quality  $x_m$  for fixed mass flux  $G$  and quality change  $\Delta x$ .

that amounts to 1.58 (this result noticeably differs from thermal performance of R22, reported by the authors in [14], which is characterized by enhancement-factor values 70% higher on average). Data for the HVA-tube exhibit a more peaked trend but with lower values (the maximum is 1.38) which approach unity at  $G=356 \text{ kg/s m}^2$ ; therefore, for this microfin tube, discrepancy between heat transfer enhancement and area increase, that amounts to 1.84, becomes relevant. Since the VA- and HVA-tubes have quite similar geometries which essentially differ only in the fin number, we infer that a large number of fins decrease the enhancement in condensation, in accordance with the findings of Yasuda et al. [5]; moreover, geometry can affect negatively fluid dynamics and heat transfer. Finally, from the thermal standpoint, Figure 4 clearly shows the superiority of the VA geometry with respect to the HVA geometry.

Figure 5 displays the dependence of  $h_c$  on the quality change  $\Delta x$  at  $x_m=0.5$  and  $G=222 \text{ kg/s m}^2$  for the smooth tube and the micro-fin tubes. As seen, the trends are essentially flat and therefore  $h_c$  is quite independent of  $\Delta x$ . Figure 6, instead, shows the influence of the average quality  $x_m$  on  $h_c$  at  $G=222 \text{ kg/s m}^2$  and  $\Delta x=0.2$ . For all the tubes the heat transfer coefficients increase with quality, as typical in-tube condensation behavior. However, for the smooth tube, the heat transfer coef-

ficient is an almost linear increasing function of the average quality while, for both the micro-fin tubes,  $h_c$  exhibits at  $x_m=0.6$  a change of slope which becomes steeper. The slope increase implies that heat transfer augmentation is larger at high values of average quality, i.e., in the annular flow. The enhancement factor, not shown, displays an increasing trend with  $x_m$  similar for both the micro-fin tubes but ranging between 1.4 and 1.8 for the VA-tube, and between 1.4 and 1.7 for the HVA-tube.

In Figure 7 data of the pressure drop per unit length  $\Delta p_c/L$  are plotted versus the mass flux  $G$  obtained for the same conditions reported in Figure 3 ( $x_{in}=0.8$  and  $\Delta x=0.6$ ). As seen, pressure gradients are considerably higher for both the micro-fin tubes than for the smooth one. Moreover, the HVA-tube exhibits pressure gradients on the average slightly lower than VA-tube. This result is clearly displayed in Figure 8 where the penalty factor, defined as the ratio of the pressure drop in the micro-fin tube to that in the smooth tube, is plotted versus  $G$ . It appears that the penalty factor decreases with increasing the mass flux. Finally, pressure gradient is quite sensitive to variations of quality but weakly dependent on quality change; in both the cases, the data obtained for the same conditions reported in Figures 4 and 5 exhibit an increasing trend with both  $x_m$  and  $\Delta x$ .

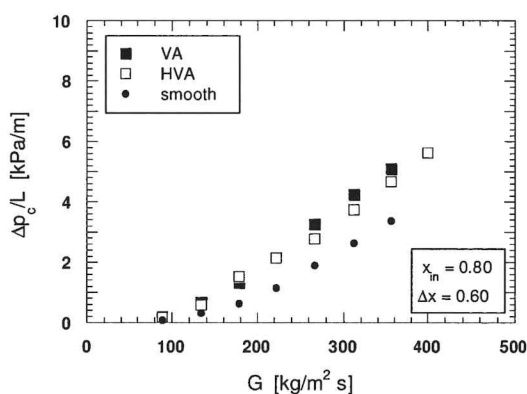


Figure 7. Pressure drop per unit length versus mass flux  $G$  for fixed inlet quality  $x_{in}$  and quality change  $\Delta x$ .

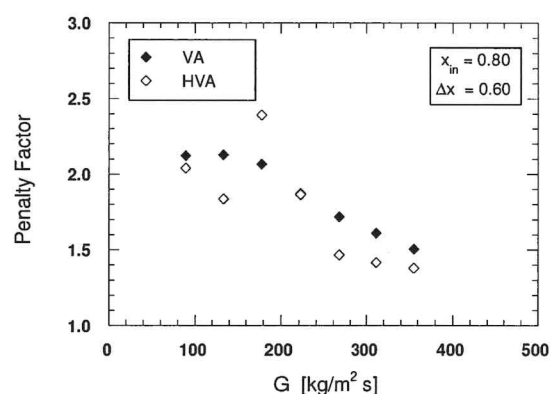


Figure 8. Penalty factor versus mass flux  $G$  for fixed inlet quality  $x_{in}$  and quality change  $\Delta x$ .

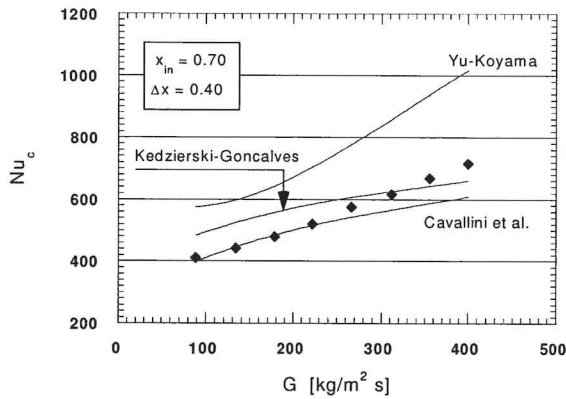


Figure 9. Experimental and calculated Nusselt number  $Nu_c$  versus mass flux  $G$  for fixed  $x_{in}$  and quality change  $\Delta x$ .

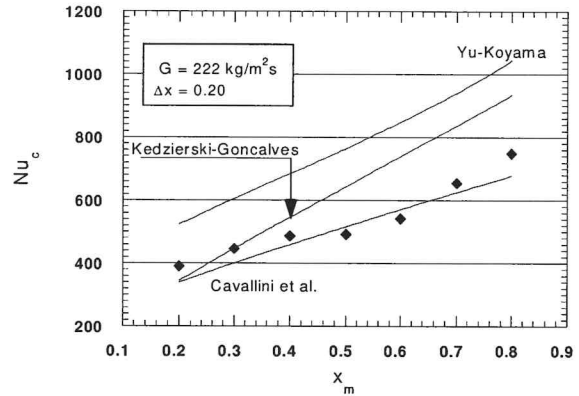


Figure 10. Experimental and calculated Nusselt number  $Nu_c$  versus average quality  $x_m$  for fixed mass flux and quality change.

COMPARISON WITH CORRELATIONS

Several correlations for condensation of refrigerants inside enhanced tubes were selected from the literature to carry out comparisons with the present data for the VA-tube. For heat transfer, the correlations of Kedzierski and Goncalves [10], Yu and Koyama [11], and Cavallini et al. [13] are considered whereas the pressure drop data are compared to the predictions obtained by the correlations of Haraguchi et al. [8], Kedzierski and Goncalves [10], Cavallini et al. [13], and Nozu et al. [15]. Figure 9 compares the experimental and predicted Nusselt numbers plotted as function of the mass flux  $G$ , obtained at  $x_{in}=0.7$  and  $\Delta x=0.4$ . In Figure 10, the calculated Nusselt numbers are compared with the experimental data in a plot versus the average quality  $x_m$ ; these values are for  $G=222 \text{ kg/m}^2\text{s}$  and  $\Delta x=0.2$ , i.e., the same conditions of Figure 6. As can be seen, the predictions of the Cavallini et. al. correlation agree very well with the data and are more correct in trend than those obtained with correlations of Kedzierski and Goncalves, and of Yu and Koyama. With the Cavallini et al. correlation, all of the data are predicted within  $\pm 20\%$ , with a mean deviation  $E=3.4\%$  and a standard deviation  $\sigma=6.5\%$ . The most significant deviations occur at high mass flux, where the correlation tends to underpredict the experimental data. The mean deviation and the standard deviation of the Kedzierski and Goncalves correlation are 13.5 and 15 percent, respectively. This correlation tends to overpredict the experimental data, particularly at high average vapour quality and at low mass fluxes. The Yu and Koyama correlation is the worst predictor of the data with a mean deviation  $E=43.3\%$  and the standard deviation  $\sigma=12.8\%$ . This correlation consistently overpredicts all of the data with a deviation that exceeds 50% for some data.

Attention is now turned to the comparison of pressure drop results. Figures 11 and 12 compare the measured values of pressure drop with the predictions of the correlations as a function of  $G$  and  $x_m$ , respectively. The experimental conditions are the same as for Figures 9 and 10. It can be noticed, that none of the correlations satisfactorily predict the pressure drop. The Haraguchi correlation proves to be the best predictor with a mean deviation of  $-24.0$  percent and a standard deviation of 11.4 percent, though it tends to underpredict the experimental data. The same tendency is exhibited also by the correlations of Cavallini et al. ( $E=-33.9\%$  and  $\sigma=23.1\%$ ) and of Kedzierski and Goncalves ( $E=-40.5\%$  and  $\sigma=15.8\%$ ). On the contrary, the Nozu correlation overpredicts the data because they exhibit a mean deviation of 26.0% with a  $\sigma=17.5\%$ ; despite this rather high deviation, though, the predictions of the correlation prove to be correct in trend.

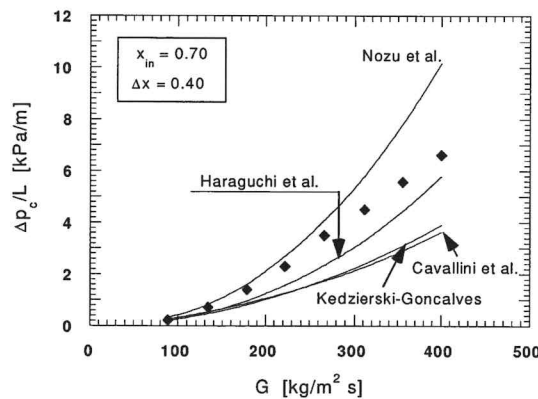


Figure 11. Experimental and calculated pressure drop per unit length versus mass flux  $G$  for fixed  $x_{in}$  and quality change  $\Delta x$ .

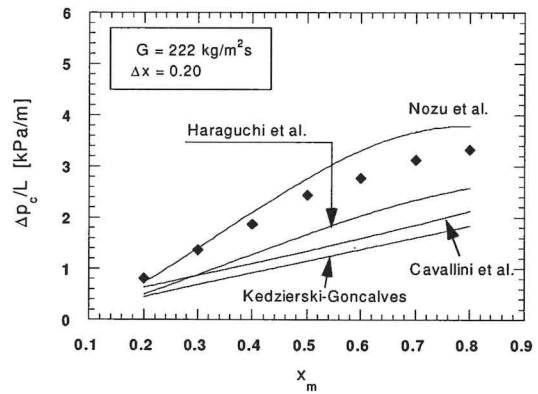


Figure 12. Experimental and calculated pressure drop per unit length versus average quality  $x_m$  for fixed  $G$  and  $\Delta x$ .

## CONCLUSIONS

Heat transfer coefficient during convective condensation of the refrigerant R134a both in smooth and micro-fin tubes is quite sensitive to variations of mass flux  $G$  and average quality  $x_m$ , exhibiting with both of them an increasing trend, but it is a weakly dependent function of the quality change  $\Delta x$ . Results for heat transfer coefficient in the micro-fin HVA-tube are lower than those in the VA-tube. The enhancement factor as a function of  $G$  displays a maximum and varies between 1.5 and 1.25 for VA-tube, and from 1.4 to approximately 1 for the HVA-tube. As a function of  $x_m$ , instead, the enhancement factor exhibits an increasing trend with values within 1.4 and 1.8 for the VA-tube, and within 1.4 and 1.7 for the HVA-tube. Consequently, the VA-tube exhibits thermal performances better than the HVA-tube; since their geometries are essentially the same excepted the fin number, we infer that a large number of fins decrease the enhancement in condensation.

Regarding pressure drop, the VA-tube shows values on the average slightly higher than those of the HVA-tube, when comparison is made at the same values of  $G$ ,  $x_m$  and  $\Delta x$ . The penalty factor is a decreasing function of  $G$  for both the micro-fin tubes.

Data for the VA-tube are compared to predictions of some correlations recently proposed for enhanced tubes. For heat transfer, the Yu and Koyama correlation consistently overpredicts the present data with a mean deviation of 43.3%; on the contrary, with the Cavallini et al. correlation, all of the data are predicted within  $\pm 20\%$  with  $E=3.9\%$  and  $\sigma=6.5\%$ . Finally, the Kedzierski and Goncalves correlation tends to overpredict the data particularly at high  $x_m$  and at low  $G$  ( $E=13.5\%$  and  $\sigma=15\%$ ). For pressure drop, none of the correlations here considered (Haraguchi, Kedzierski and Goncalves, Cavallini, and Nozu) satisfactorily predict our data. The Haraguchi correlation, though it tends to underpredict data, proves to be the less inaccurate predictor with  $E=-24.0\%$  and  $\sigma=11.4\%$ .

## ACKNOWLEDGEMENTS

This work is supported by MURST (the Italian Department for the University and for the Scientific and Technical Research) via COFIN 2001 grants.

## REFERENCES

- Schlager L.M., Bergles A.E., Pate M.B., "A survey of refrigerant heat transfer and pressure drop emphasizing oil effects and in-tube augmentation", *ASHRAE Trans.*, vol. 93, Pt. 1, 1987.
- Schlager L.M., "Boiling and Condensation in Micro-fin Tubes", in "Industrial Heat Exchangers", Lecture Series 1991-04, von Karman Institute for Fluid Dynamics, Belgium, 1991.
- Webb, R.L., "Principles of Enhanced Heat Transfer", John Wiley & Sons, Inc., New York, 1994.
- Schlager L.M., Pate M.B., Bergles A.E., "Evaporation and condensation heat transfer and pressure drop in horizontal, 12.7-mm micro-fin tubes with refrigerant 22", *J. Heat Transfer* **112**, pp. 1041-1047, 1990.
- Yasuda K., Ohizumi K., Hori M. and Kawamata o., "Development of condensing thermofin-HEX-C tube", *Hittachi Cable Rev.*, **9**, pp. 27-30, 1990.
- Chiang R., "Heat Transfer and pressure drop during evaporation and condensation of refrigerant-22 in 7.5 mm diameter axial and helical grooved tubes", *A. I. Ch. E. Symp. Ser.* **295**, **89**, pp. 205-210, 1993.
- Eckels, S.J., Pate, M.B., "Evaporation and Condensation of HFC-134a and CFC-12 in a Smooth Tube and a Micro-fin Tube", *ASHRAE Trans.*, vol. 97, Pt. 2, 1991
- Haraguchi H., Koyama S., Esaki J., Fujii T., "Condensation heat transfer of refrigerants HFC134a, HCFC123 and HCFC22 in a horizontal smooth tube and a horizontal micro-fin tube", *Proc. 30<sup>th</sup> Nat. Symposium of Japan, Yokohama*, pp. 343-345, 1993.
- Dobson M.K., Chato J.C., "Experimental evaluation of internal condensation of refrigerants R12 and R134a", *ASHRAE Trans.*, vol. 100, Pt.2, pp. 744-754, 1994.
- Kedzierski M.A., Goncalves J.M., "Horizontal condensation of alternative refrigerants within a micro-fin tube", NISTIR 6095, US Department of Commerce, 1997.
- Yu Y., Koyama S., "Condensation heat transfer of pure refrigerants in micro-fin tubes", *Proc. Int. Refrigeration Conference at Purdue*, pp. 325-330, 1998.
- Eckels S.J., Tesene B.A., "A comparison of R22, R134a, R410A and R407C condensation performance in smooth and enhanced tubes: Part I, Heat transfer", *ASHRAE Trans.*, vol. 105, Pt. 2, 1999.
- Cavallini A., Del Col D., Doretti L., Longo G.A., Rossetto L., "Heat transfer and pressure drop during condensation of refrigerants inside horizontal enhanced tubes", *Int. J. of Refrigeration*, vol. 23, pp. 4-25, 2000.
- Muzzio A., Niro A., "Condensation of R134a inside a new microfin tube". *Proc. 20th Heat Transfer National Conference of Italy*, pp. 265-270, 2002.
- Nozu S., Katayama H., Nakata H., Honda H., "Condensation of refrigerant CFC11 in horizontal micro-fin tubes (proposal of a correlation equation for frictional pressure gradient)", *Experimental Thermal and Fluid Sciences*, vol. 18, pp. 82-96, 1998.